

Experimental study of holographic generation of fractional Bessel beams

Shao Hua Tao, Woei Ming Lee, and Xiaocong Yuan

We demonstrate the experimental generation of a fractional Bessel beam by holographic means. Such fractional modes of Bessel beams possess an intrinsic opening gap across concentric intensity rings on propagation. We also show that the opening gaps within the fractional modes are diffraction free for a working distance while a fractional helical wave front is maintained. © 2004 Optical Society of America
OCIS codes: 050.1970, 090.0090, 140.7010.

1. Introduction

Both zero-order and higher-order Bessel beams are well known as nondiffracting beams.¹ As a result, they have been used for optical alignment, surveying, and data storage. In recent years a new application of Bessel beams has generated much interest in the area of optical micromanipulation. In this field the characteristics of the Bessel beams, one of which is their self-reconstructing ability, have been fully exploited, as Bessel beams are able to trap multiple microparticles separated in different planes.² Apart from the properties mentioned above, higher-order Bessel beams possess an extra characteristic, which is a helical phase wave front.³ This extra property of the beams allows it to transfer orbital angular momentum to the microparticles. Bessel beams have therefore been used for optical trapping and guiding.^{4–6}

It is known that axicons and holograms are two common devices that can be used to produce Bessel beams. With an axicon, when a plane wave passes through a conical lens the beam will be transformed into a zero-order Bessel beam.⁷ Similarly, shining a higher-order Laguerre–Gaussian beam through the axicon then transforms the beam into a higher-order Bessel beam.⁸ The nondiffraction distance of the Bessel beam is determined to a large extent by the tip

angle of the axicon and by the beam size of the incident light shining onto the axicon. Such a method of generating Bessel beams has high optical efficiency; however, an axicon lacks flexibility and requires stringent alignment. Furthermore, to produce a higher-order Bessel beam it is necessary to generate a corresponding-order Laguerre–Gaussian beam as an incident wave front for the axicon.

Turunen *et al.*⁹ reported a holographic method for generating Bessel beams. A hologram can generate the same phase values as the phase retardation produced by the axicon with which to reconstruct a zero-order Bessel beam. Similarly, a hologram whose phase simulates the superposition of the axicon phase distribution and a higher-order helical phase distribution can also generate a higher-order Bessel beam.^{10,11} The holographic method gives much flexibility in generating Bessel beams with various beam coefficients and orders, and the system is simple and compact.

However, the Bessel beams described above are assumed to have integer orders; i.e., the amplitude of the beam is an integer order of the Bessel function of the first kind, and the helical phase order is also set as the same integer. In this paper we investigate the unique properties of fractional orders as used for both amplitude and phase of the Bessel beams, to which we refer as fractional Bessel beams (FBBs).

Computer-generated holograms, which are produced by some phase-retrieval algorithms, can modulate the phases of the incident beams to yield predefined amplitude or phase distributions. However, it is difficult for a single computer-generated hologram obtained by a phase-retrieval algorithm to customize a reconstructed beam in amplitude and phase simultaneously.

Recently we reported the dynamic generation of a

The authors are with the Photonics Research Centre, School of Electrical and Electronic Engineering, Nanyang Technological University, Nanyang Avenue, Singapore 639798. X. Yuan's e-mail address is excyuan@ntu.edu.sg.

Received 10 July 2003; revised manuscript received 23 September 2003; accepted 6 October 2003.

0003-6935/04/010122-05\$15.00/0

© 2004 Optical Society of America

FBB by a spatial light modulator (SLM).¹² The FBB was generated by use of a simulated axicon with a fractional helical phase. In this paper we propose a method with which to utilize the amplitude of a fractional-order Bessel function coupled with the appropriate fractional order of a helical phase such that the resultant FBB has high purity. We use an interference method to generate the FBB. Such a method is simple and cost effective, and it has been applied widely to generate holograms.¹³ With this method we reconstruct a pure FBB, i.e., an amplitude and a phase with the same order. The experimental results demonstrate that the quality of the FBB intensity patterns produced in this way are better than that of patterns generated by the axicon-approximation method.

2. Description of Fractional Bessel Beams

As we know, the complex amplitude of an n th order Bessel beam on plane $z = 0$ mm is given by

$$E_{\pm n}(\rho, \phi) = J_n(\alpha\rho)\exp(\pm in\phi), \quad (1)$$

where J_n is the n th Bessel function of the first kind, ρ is the transverse spatial coordinate, ϕ is an azimuthal phase, and α is an adjustable constant of the Bessel function, which represents the radial component of the free-space wave vector of the beam. When order n is an integer, the distribution is an integer-order Bessel beam (IBB), but, if the order is set to a positive fractional number, the distribution of Eq. (1) will become a FBB.

Simply changing the value of n will cause the resultant Bessel beam to possess different intensity distributions. A higher-order Bessel beam, for integer values of n , will have a dark circular spot in the center, and the outer concentric rings will remain the same, whereas the fractional orders between two adjacent integer orders of Bessel beams will have opening slits with various widths. For clearer observation, we chose a much higher-order Bessel beam, $n = 4.5$ with which to demonstrate the properties of the FBBs. The intensity profile and the phase distribution of the beam on plane $z = 0$ mm are shown in Fig. 1. The size of the beam is approximately 3.84 mm by 3.84 mm. Parameter α in J_n is given as 13 1/mm.

The intensity and the phase distributions of an IBB with $n = 4$ are shown in Fig. 2 and have the same parameters as FBB shown in Fig. 1, except for the order.

It can be seen from Figs. 1 and 2 that the two intensity profiles are similar, except for the sizes of the central dark spots. Their intensity rings are fully closed, with no opening. However, their phase distributions are much different. The 4th-order Bessel beam has eight arc sections distributed evenly from the innermost to the outermost ring. The fractional beam, however, has nine arc sections. In the central parts of the two phase patterns there are four arms distributed evenly in the IBB, whereas there are four arms and one incomplete arm in the FBB.

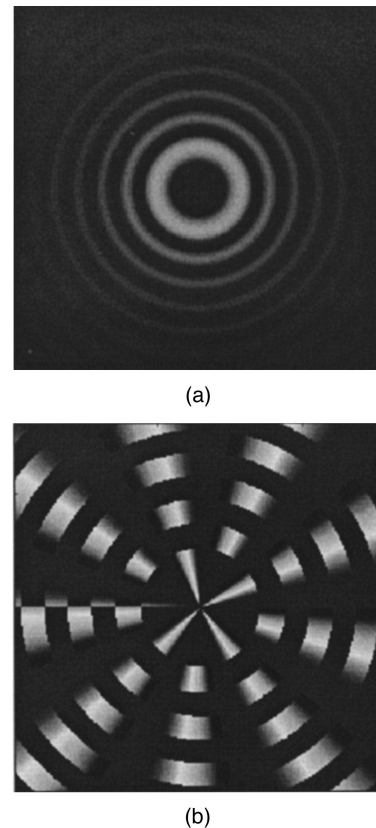


Fig. 1. FBB at $z = 0$ mm and $n = 4.5$: (a) intensity, (b) phase.

The intensity differences between the FBB and the IBB can be clearly observed as the beam propagates in free space. We can calculate their distributions at a propagation distance z by using the Fresnel diffraction integral.¹⁴ The FBB and the IBB on the plane $z = 300$ mm are shown in Fig. 3. The outer rings in Fig. 3 appear rather square because of the tailored square beam profile in the simulation.

In Fig. 3 the FBB has radial gaps in its concentric intensity rings, whereas the IBBs are fully closed rings. However, the sizes of the intensity rings are nearly unchanged, and more simulations and experiments showed that both kinds of rings are diffraction free within this distance.

3. Holographic Generation of Fractional Bessel Beams

To produce a FBB experimentally, we caused interference between a reference plane wave and a desired FBB to generate a hologram. The hologram's phase data were then loaded in a SLM. Thus, when a reference plane wave was incident upon the SLM, the object was reconstructed. To verify the simulation result, we continued to use the FBB ($n = 4.5$) and a plane wave to generate the hologram. To separate the reconstructed images of different orders, we used an oblique plane wave $\{p = \exp[i2\pi(x/d)\delta]\}$, where δ is an adjustable constant that was set as 121 here. d is the pixel width of the SLM to be the reference light. The resultant hologram is shown in Fig. 4.

The phase data of the hologram were subsequently

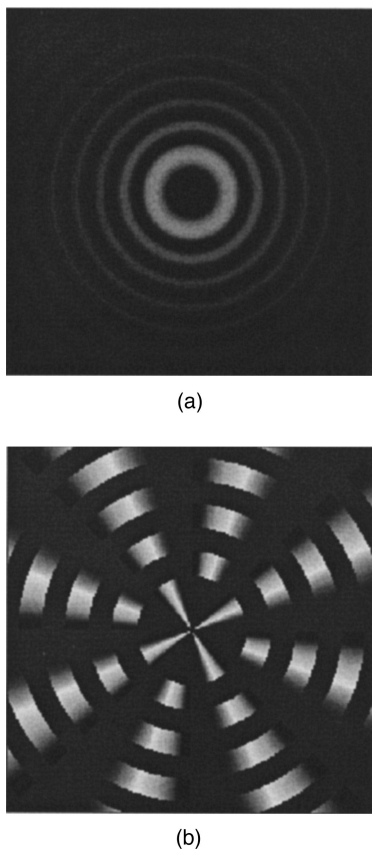


Fig. 2. IBB at $z = 0$ mm and $n = 4$: (a) intensity, (b) phase.

saved as a gray-scale image file. The different gray scales of the image correspond to different phase values. We then used a SLM to reconstruct the FBB. The SLM from the Boulder Nonlinear System¹⁵ is a nematic type that works on reflection, which can have more than 64 phase strokes. A schematic of the reconstruction system is shown in Fig. 5.

Figure 5 shows a He-Ne laser beam with wavelength 632.8 nm expanded by a collimation system and then projected onto a SLM screen. The loaded hologram data in the SLM have 512 by 512 sampling points, and each pixel size of the SLM is 15 μm by 15 μm . The hologram has been quantized to 32 levels. The reflected light is received by a Beamstar-1500 CCD beam profiler. We measured the reconstructed patterns at different distances from the beam profiler. The intensity profiles of the beam are shown in Fig. 6.

The overall sizes of the patterns in Fig. 6 are approximately 3.84 mm by 3.84 mm. The intensity profiles observed in the form of an elliptical shape in the figures are due to the aspect ratio of the CCD camera. The FBB is diffraction free along the propagation distance from $z = 0.3$ to $z = 0.5$ m, as shown in Figs. 6(a) and 6(b), which is considered long enough for a micromanipulation application. The IBB's nondiffracting distance with the same beam parameters is ~ 0.7 m. Beyond the nondiffraction range the size of the innermost ring is almost unchanged at $z = 0.6$ m and $z = 1.0$ m in Figs. 6(c) and

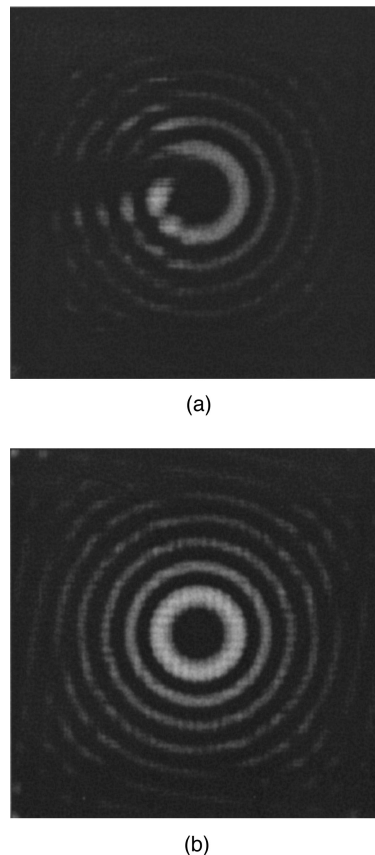


Fig. 3. Diffraction intensity distributions of the FBB and the IBB: (a) FBB of $n = 4.5$ at $z = 300$ mm, (b) IBB of $n = 4$ at $z = 300$ mm.

6(d), but the orientation of the openings rotates with the beam's propagation. Such rotation of the optical beam's intensity has been attributed to the helical wave front of the beam.¹⁶

To further illustrate the existence of the helical phase of the FBBs we employed the method of interference between two FBBs of opposite helicity such that we could observe their phases. Hence, two different diffracted orders (the first and the minus first of the hologram) of the 4.5th-order Bessel beam were redirected by a Michelson interferometer¹⁷ to inter-

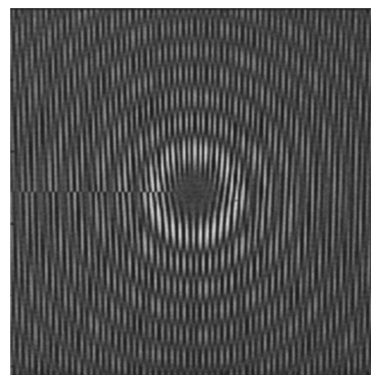


Fig. 4. Hologram produced by the interference of the FBB of $n = 4.5$. The gray scales represent different phase values. The phase is quantized into 32 levels.

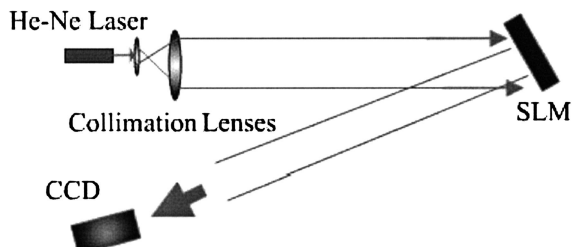


Fig. 5. Schematic of the experimental setup.

ferre on the plane at a distance $z = 1$ m from the SLM plane. Simulations of the interference of the IBBs and the FBBs are presented in Figs. 7(a) and 7(b), respectively. In the experiment the interference fringes were recorded by a CCD camera; they are shown in Fig. 7(c). The interference fringes from $n = 4$ through $n = -4$ are shown in Fig. 7(d).

It can be seen from Fig. 7 that both interference patterns have forklike fringes, which confirms the existence of helical azimuthal phase variations in FBBs and IBBs. For the IBBs it was proved that the helical phase induced an orbital angular momentum. This could provide an analogy with the FBBs. In Figs. 7(a) and 7(b) the brightest rings in both patterns are composed of many petals, but one of the petals in the FBB caused by the FBB's fractional helical wave front is not observed clearly in the figure because of the fractional Bessel amplitude of the fractional beam.

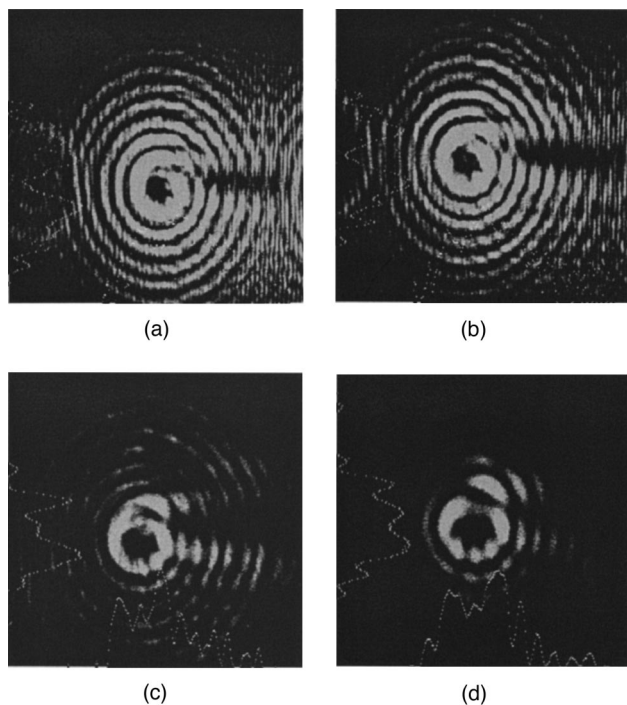


Fig. 6. Reconstructed FBB intensity patterns at several distances z from the SLM, $n = 4.5$: (a) $z = 0.3$ m, (b) $z = 0.5$ m, (c) $z = 0.6$ m, (d) $z = 1$ m.

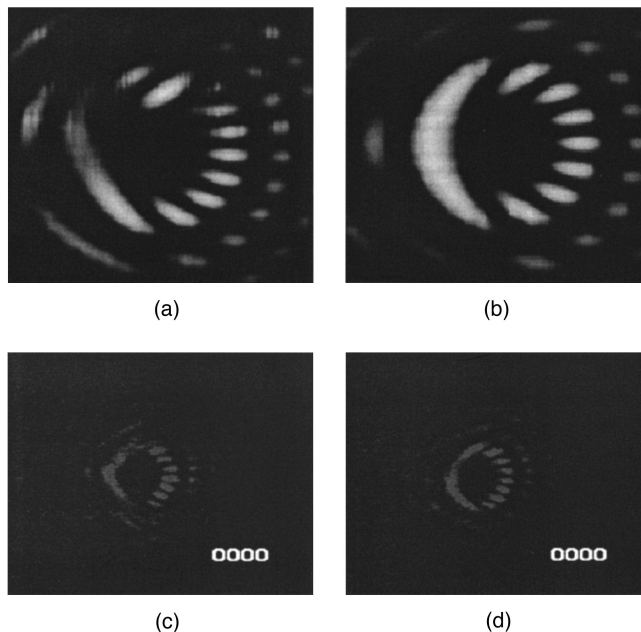


Fig. 7. Interference patterns at $z = 1$ m: (a) simulation of interference, $n = 4.5$ and $n = -4.5$, (b) simulation of interference, $n = 4$ and $n = -4$, (c) experimental interference, $n = 4.5$ and $n = -4.5$, (d) experimental interference, $n = 4$ and $n = -4$.

4. Conclusions

In conclusion, we have shown experimentally the propagation of fractional Bessel beams, especially of order 4.5, by holographic means. We have also shown that the reconstructed FBB not only is diffraction free but also maintains its helical phase wave front. Moreover, we demonstrated that the opening slit in its concentric intensity rings is distinctly different from that of the integer-order Bessel beams.

We have shown a clear and simple method of obtaining a FBB by using a single optical element. Experimental generation of the FBB has been shown to be in good agreement with the simulation results.

The main use of a FBB can best be described as its use as a dark optical trap for confining neutral atoms.^{5,6} Rhodes *et al.*⁵ have shown that the obstructed guide, which creates artificial openings, increases coupling efficiency. They also mentioned that higher coupling efficiency into an obstructed Laguerre–Gaussian beam and a high-order Bessel beam can be achieved, for instance, by dropping a magneto-optic trap cloud under gravity into an oblique guide.

Hence it is not difficult for us to see the FBB's potential usefulness for trapping neutral atoms. The openings from the FBB create a clear opening in a hollow beam with a diffractionless distance that is not easily attainable by other means. Hence this FBB can be a great alternative to the obstructed guide of Rhodes *et al.*⁵

References

1. J. Durnin, J. J. Miceli, Jr., and J. H. Eberly, "Diffraction-free beams," *Phys. Rev. Lett.* **58**, 1499–1501 (1987).

2. V. Garces-Chavez, D. McGloin, H. Melville, W. Sibbett, and K. Dholakia, "Simultaneous micromanipulation in multiple planes using a self-reconstructing light beam," *Nature* **419**, 145–147 (2002).
3. K. Volke-Sepulveda, V. Garces-Chavez, S. Chavez-Cerda, J. Arlt, and K. Dholakia, "Orbital angular momentum of a high-order Bessel light beam," *J Opt. B* **4**, S82–S89 (2002).
4. J. Arlt, V. Garces-Chavez, W. Sibbett, and K. Dholakia, "Optical micromanipulation using a Bessel light beam," *Opt. Commun.* **197**, 239–245 (2001).
5. D. P. Rhodes, G. P. T. Lancaster, J. Livesey, D. McGloin, J. Arlt, and K. Dholakia, "Guiding a cold atomic beam along a co-propagating and oblique hollow light guide," *Opt. Commun.* **214**, 247–254 (2002).
6. M. Florjańczyk and R. Tremblay, "Guiding of atoms in a traveling-wave laser trap formed by the axicon," *Opt. Commun.* **73**, 448–450 (1989).
7. G. Scott and M. McArdle, "Efficient generation of nearly diffraction-free beams using an axicon," *Opt. Eng.* **31**, 2640–2643 (1992).
8. J. Arlt and K. Dholakia, "Generation of high-order Bessel beams by use of an axicon," *Opt. Commun.* **177**, 297–301 (2000).
9. J. Turunen, A. Vasara, and A. T. Friberg, "Holographic generation of diffraction-free beams," *Appl. Opt.* **27**, 3959–3961 (1988).
10. A. Vasar, J. Turunen, and A. T. Friberg, "Realization of general nondiffracting beams with computer-generated holograms," *J. Opt. Soc. Am A* **6**, 1748–1754 (1989).
11. J. A. Davis, J. Guertin, and D. M. Cottrell, "Diffraction-free beams generated with programmable spatial light modulators," *Appl. Opt.* **32**, 6368–6370 (1993).
12. S. H. Tao, W. M. Lee, and X.-C. Yuan, "Dynamic optical manipulation with a higher-order fractional Bessel beam generated from a spatial light modulator," *Opt. Lett.* **28**, 1867–1869 (2003).
13. M. P. MacDonald, L. Paterson, K. Volksepulveda, J. Arlt, W. Sibbett, and K. Dholakia, "Revolving interference patterns for rotation of optically trapped particles," *Opt. Commun.* **201**, 21–28 (2002).
14. J. W. Goodman, *Introduction to Fourier Optics*, 2nd ed. (McGraw-Hill, New York, 1996).
15. "512 × 512 multi-level/analog liquid crystal spatial light modulator" (Boulder Nonlinear System, Lafayette, Colo.), [http: www.bnnonlinear.com/pages/512slm.html](http://www.bnnonlinear.com/pages/512slm.html).
16. J. Arlt, "Handedness and azimuthal energy flow of optical vortex beams," *J. Mod. Opt.* **50**, 1573–1580 (2003).
17. W. M. Lee, X.-C. Yuan, and D. Y. Tang, "Optical tweezers with multiple optical forces using double hologram interference," *Opt. Exp.* **11**, 199–207 (2003), <http://www.opticsexpress.org>.